Density Functional Theory Study on Anti-resonance in Preresonance Raman Scattering for Naphthalene Molecules

Ren-Hui Zheng*,† and Wen-Mei Wei‡

School of Life Science, University of Science and Technology of China (USTC), Hefei, Anhui, 230026, People's Republic of China, and Department of Chemistry, College of Basic Medicine, Anhui Medical University, Hefei, Anhui, 230032, People's Republic of China

Received: December 26, 2006; In Final Form: February 24, 2007

The anti-resonance phenomenon in preresonance Raman scattering is investigated on the basis of the direct Taylor expansion of the electric dipole transition moments in vibrational Raman tensors with respect to vibrational normal coordinates. A time-dependent density functional theory treatment is applied to compute the anti-resonance of a nontotally symmetric vibrational model for naphthalene molecules, and the model spectra agree favorably with experiment. This direct evaluation approach may provide a method of predicting anti-resonance and studying its origin.

1. Introduction

For resonance Raman scattering there is a rapid change in Raman scattered intensity as the exciting frequency is scanned across the various absorption bands, and analyses of Raman excitation profiles often provide structural information and vibronic coupling on electronic excited states.[1] Raman excitation profiles usually show increasing intensity when the incident frequency is moved toward resonance. The opposite behavior, that is, an increase in the frequency of the laser reducing the Raman intensity, is named anti-resonance. This phenomenon has been observed for a nontotally symmetric vibration in naphthalene[2−4] and anthracence,[3,5] which show a hidden anti-resonance for symmetric vibration followed by a strong polarization dispersion,[4] and for both totally and nontotally symmetric modes in some transition metal complexes,[6] some benzene derivatives,[7] trans-azobenzene,[8] and methylpyridines.[9]

Theories have been applied to explain the anti-resonance. Stein et al.[6−8] pointed out that the anti-resonance is ascribable to a destructive interference between the weak scattering from the forbidden electronic states and the strong preresonance scattering from the higher energy allowed electronic states. In 1977, Zgierski[10] derived a simple closed formula of the interference effects in the preresonance Raman region for the cross section of a totally symmetric fundamental line where the vibrational structure of electronic transitions is smeared out. In 1981, Robinson et al.[11,12] found the anti-resonance scattering within a theory built on the velocity representation of the scattering tensor taking into account only one electronic state and only the Franck−Condon term. In 1982, Hassing and Svendsen[13] studied the interference between the Franck−Condon and Herzberg−Teller terms in the preresonance scattering region for a totally symmetric mode. In 1997, Hassing[14] explained the anti-resonance phenomenon in the preresonance Raman scattering of an allowed electronic transition for both totally and nontotally symmetric modes in terms of an analytical model and presented the necessary and general conditions for obtaining an anti-resonance.

Though experiments and theories have been carried out, an ab initio investigation of anti-resonance has not been reported. Just as Hassing point out,[14] one of the practical difficulties in using the Raman excitation spectra to gain information about the molecular parameters is the limited number of experimental points normally obtained combined with the relative large numbers of model parameters. Quantum computations are helpful to overcome some of those difficulties, which can obtain many molecular parameters such as excitation wavefunctions, excitation energies, electric dipole transition moments, and their derivatives. Furthermore, a computational investigation is highly desirable for a detailed theoretical study and prediction on the anti-resonance phenomenon.

In this paper, we do an ab initio study on anti-resonance for Raman scattering in the preresonance region. In section 2, the expression for vibrational Raman polarizabilities in the preresonance region is presented in a direct Taylor expansion scheme, then the Warshel and Dauber calculation method[15−18] of electric dipole transition moment derivatives with respect to normal coordinates is applied to analyze anti-resonant vibrational Raman polarizabilities. In section 3, on the basis of the above formulas and a time-dependence density functional theory computation TDDFT//B3LYP/AUG-cc-pVDZ with the Gaussian 98 package, we calculate the anti-resonance excitation profiles for the b_{3g} vibrational mode at 1629 cm^{-1} for naphthalene molecules. The model spectra compare favorably with experiment data. This direct evaluation approach may provide a way of predicting anti-resonance Raman scattering and studying its origin.

2. Theory

For Raman measurements of randomly oriented scattering systems with linearly polarized light, in a 90° arrangement, the differential scattering cross sections with the scattered radiation polarized parallel and perpendicular to the polarization of the incoming beam are given

* Author to whom correspondence should be addressed. E-mail: zrh@ustc.edu.
† University of Science and Technology of China.
‡ Anhui Medical University.

10.1021/jp068930d CCC: $37.00
Published on Web 04/18/2007

respectively by[1,14]

$$\left(\frac{d\sigma}{d\Omega}\right)_{||} = 4\pi^2\alpha^2\nu_s^4\left[\frac{1}{30}(10\Sigma^0 + 4\Sigma^2)\right] \quad (1)$$

$$\left(\frac{d\sigma}{d\Omega}\right)_{\perp} = 4\pi^2\alpha^2\nu_s^4\left[\frac{1}{30}(5\Sigma^1 + 3\Sigma^2)\right] \quad (2)$$

where α is the fine structure constant, υ_s is the frequency of the scattered light. Placzek isotropic, antisymmetric, and anisotropy tensor invariants Σ^0, Σ^1, and Σ^2 are defined as

$$\Sigma^0 = \frac{1}{3}|\alpha_{xx} + \alpha_{yy} + \alpha_{zz}|^2$$

$$\Sigma^1 = \frac{1}{2}\{|\alpha_{xy} - \alpha_{yx}|^2 + |\alpha_{xz} - \alpha_{zx}|^2 + |\alpha_{yz} - \alpha_{zy}|^2\}$$

$$\Sigma^2 = \frac{1}{2}\{|\alpha_{xy} + \alpha_{yx}|^2 + |\alpha_{xz} + \alpha_{zx}|^2 + |\alpha_{yz} + \alpha_{zy}|^2\} + \frac{1}{3}\{|\alpha_{xx} - \alpha_{yy}|^2 + |\alpha_{xx} - \alpha_{zz}|^2 + |\alpha_{yy} - \alpha_{zz}|^2\} \quad (3)$$

The total differential scattering cross section ($d\sigma/d\Omega$) is given by

$$\left(\frac{d\sigma}{d\Omega}\right) = \left(\frac{d\sigma}{d\Omega}\right)_{||} + \left(\frac{d\sigma}{d\Omega}\right)_{\perp} = 4\pi^2\alpha^2\nu_s^4\left[\frac{1}{30}(10\Sigma^0 + 5\Sigma^1 + 7\Sigma^2)\right] \quad (4)$$

and the depolarization ratio ρ which describes the polarization properties can be expressed into

$$\rho = \frac{\left(\frac{d\sigma}{d\Omega}\right)_{\perp}}{\left(\frac{d\sigma}{d\Omega}\right)_{||}} = \frac{5\Sigma^1 + 3\Sigma^2}{10\Sigma^0 + 4\Sigma^2} \quad (5)$$

The vibrational Raman transition polarizability tensor $\alpha_{\rho\sigma}$ in eq 3 is derived by the second-order perturbation theory[15,16,19−22]

$$\alpha_{\rho\sigma} = \frac{1}{h}\sum_{M,m}\left[\frac{\langle Gg|\mu_\sigma|Mm\rangle\langle Mm|\mu_\rho|Gg'\rangle}{(\upsilon_{Mm,Gg} - \upsilon - i\Gamma_{Mm})} + \frac{\langle Gg|\mu_\rho|Mm\rangle\langle Mm|\mu_\sigma|Gg'\rangle}{(\upsilon_{Mm,Gg'} + \upsilon + i\Gamma_{Mm})}\right] \quad (6)$$

where G and M represent the ground and excited electronic states, respectively, g, g', and m represent vibrational levels, μ_σ and μ_ρ are the electric dipole moment operators in Cartesian coordinates, $\upsilon_{Mm,Gg}$ and $\upsilon_{Mm,Gg'}$ are the frequency differences between the indicated vibronic levels, υ is the excitation light frequency, and Γ_{Mm} is the damping parameter of the Mth vibronic state.

The transition moments in eq 6 can be evaluated first by integrating over the electronic coordinates and then by expanding the integral in a Taylor series in terms of the molecular normal modes[15,16]

$$\langle G|\vec{\mu}|M\rangle = \langle G|\vec{\mu}|M\rangle_0 + \sum_t (\partial\langle G|\vec{\mu}|M\rangle/\partial Q_t)_0 Q_t + \cdots \quad (7)$$

Using eq 7, we can express eq 6 into A and B terms

$$\alpha_{\rho\sigma} = A_{\rho\sigma} + B_{\rho\sigma} \quad (8)$$

where

$$A_{\rho\sigma} = \frac{1}{h}\sum_{Mm}\left\{\frac{\langle G|\mu_\sigma|M\rangle_0\langle M|\mu_\rho|G\rangle_0}{\upsilon_{Mm,Gg} - \upsilon_0 - i\Gamma_{Mm}} + \frac{\langle G|\mu_\rho|M\rangle_0\langle M|\mu_\sigma|G\rangle_0}{(\upsilon_{Mm,Gg'} + \upsilon + i\Gamma_{Mm})}\right\} \times \bar{C}(g,m)\bar{C}(g',m) \quad (9)$$

$$B_{\rho\sigma} = \frac{1}{h}\sum_{Mm}\frac{1}{\upsilon_{Mm,Gg} - \upsilon_0 - i\Gamma_{Mm}} \times [\langle G|\mu_\sigma|M\rangle_0(\partial\langle M|\mu_\rho|G\rangle/\partial Q_t)_0\bar{C}(g,m)\bar{C}^t(g',m) + \langle G|\mu_\rho|M\rangle_0(\partial\langle M|\mu_\sigma|G\rangle/\partial Q_t)_0\bar{C}(g',m)\bar{C}^t(g,m)] + \frac{1}{h}\sum_{Mm}\frac{1}{\upsilon_{Mm,Gg'} + \upsilon_0 + i\Gamma_{Mm}} \times [\langle G|\mu_\rho|M\rangle_0(\partial\langle M|\mu_\sigma|G\rangle/\partial Q_t)_0\bar{C}(g,m)\bar{C}^t(g',m) + \langle G|\mu_\sigma|\mathrm{M}\rangle_0(\partial\langle M|\mu_\rho|G\rangle/\partial Q_t)_0\bar{C}(g',m)\bar{C}^t(g,m)] \quad (10)$$

Here, $\bar{C}(g,m)$, $\bar{C}(g',m)$, $\bar{C}^t(g,m)$, and $\bar{C}^t(g',m)$ are the vibrational integrals $\langle g,m\rangle$, $\langle g',m\rangle$, $\langle g'|Q_t|m\rangle$, and $\langle g|Q_t|m\rangle$, respectively. Using the recursion formulas (see eqs 9 and 10 in ref 15 and

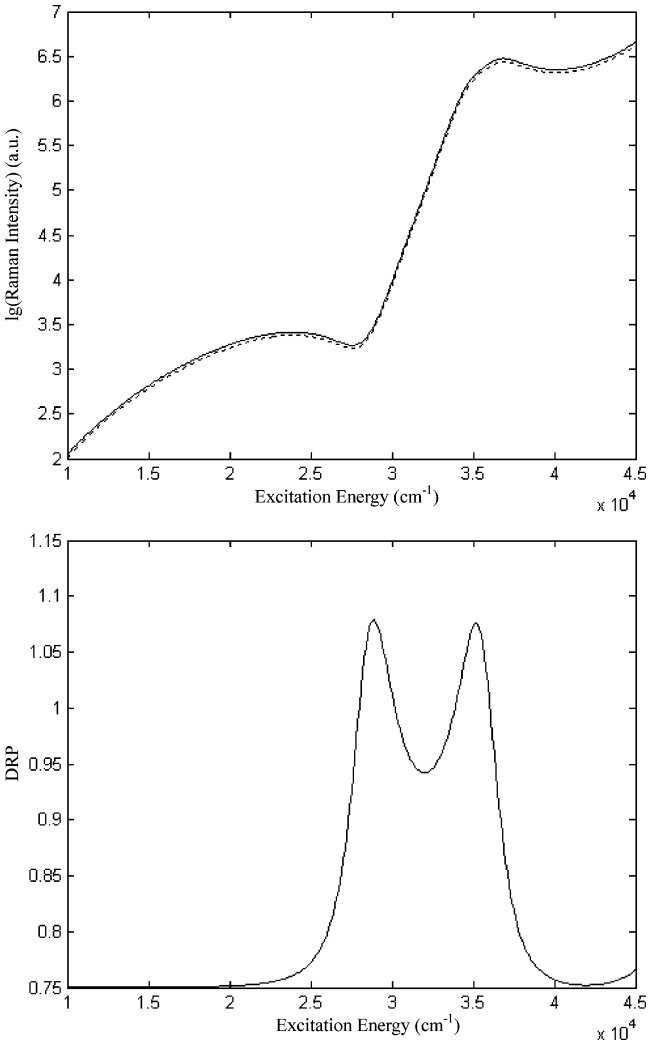

Figure 1. Calculated preresonance excitation profiles and DPR of the b_{3g} vibrational mode of naphthalene at 1629 cm^{-1} using the 100-excited-singlet-state model with the damping constant Γ = 1600 cm^{-1} and the displacement parameters $\Delta_t = 0$ (solid line) and $\Delta_t = 0.2$ (dotted line).

eqs I and II in ref 23) for the vibrational overlap integral, only considering the $m_t = 0$ and $m_t = 1$ contributions for the Q_t mode and assuming that there is no difference of vibrational wave number between the ground state and the excited states but a displacement Δ_t of the potential energy minimum along the normal coordinate Q_t and $\Delta_t \ll 1$, from ref 21, we obtain the Franck−Condon factors $\bar{C}(0_t,0_t) \approx \bar{C}(1_t,1_t) = \exp(-\Delta_t^2/2) = a$, $\bar{C}(0_t,1_t) \approx -\bar{C}(1_t,0_t) \approx -\bar{C}(2_t,1_t)/\sqrt{2} = -\Delta_t \exp(-\Delta_t^2/2) = b$, and $\sqrt{2}\,\bar{C}(0_t,0_t)\bar{C}(2_t,0_t) \approx -b^2$. Thus, eqs 9 and 10 for the fundamental Raman transitions ($g = 0$ and $g' = 1$) are respectively

$$A_{\rho\sigma} = \sum_M \frac{ab\langle G|\mu_\sigma|M\rangle_0\langle M|\mu_\rho|G\rangle_0}{h}\left\{\frac{1}{\Delta\upsilon_0 + \upsilon_t - i\Gamma_M} - \frac{1}{\Delta\upsilon_0 - i\Gamma_M}\right\} + \sum_M \frac{ab\langle G|\mu_\rho|M\rangle_0\langle M|\mu_\sigma|G\rangle_0}{h}\left\{\frac{1}{\upsilon_{MG} + \upsilon + i\Gamma_M} - \frac{1}{\upsilon_{MG} + \upsilon - \upsilon_t + i\Gamma_M}\right\} \quad (11)$$

$$B_{\rho\sigma} = \frac{1}{\sqrt{2}h}\sum_M \left[\frac{1}{\Delta\upsilon_0 - i\Gamma_M}\{(a^2 + b^2)\langle G|\mu_\sigma|M\rangle(\partial\langle M|\mu_\rho|G\rangle/\partial Q_t)_0 + b^2\langle G|\mu_\rho|M\rangle_0(\partial\langle M|\mu_\sigma|G\rangle/\partial Q_t)_0\} + \frac{1}{\Delta\upsilon_0 + \upsilon_t - i\Gamma_M}\{a^2\langle G|\mu_\rho|M\rangle_0(\partial\langle M|\mu_\sigma|G\rangle/\partial Q_t)_0 - b^2\langle G|\mu_\sigma|M\rangle(\partial\langle M|\mu_\rho|G\rangle/\partial Q_t)_0\}\right] + \frac{1}{\sqrt{2}h}\sum_M \left[\frac{1}{\upsilon_{MG} + \upsilon_0 - \upsilon_t + i\Gamma_{Mm}} \times \{(a^2 + b^2)\langle G|\mu_\rho|M\rangle(\partial\langle M|\mu_\sigma|G\rangle/\partial Q_t)_0 + b^2\langle G|\mu_\sigma|M\rangle_0(\partial\langle M|\mu_\rho|G\rangle/\partial Q_t)_0\} + \frac{1}{\upsilon_{MG} + \upsilon_0 + i\Gamma_{Mm}}\{a^2\langle G|\mu_\sigma|M\rangle_0(\partial\langle M|\mu_\rho|G\rangle/\partial Q_t)_0 - b^2\langle G|\mu_\rho|M\rangle(\partial\langle M|\mu_\sigma|G\rangle/\partial Q_t)_0\}\right] \quad (12)$$

It is clear that $b = 0$ if the vibrational mode is nontotally symmetric; that is, Raman A terms (eq 11) do not contribute to the nontotally symmetric vibrational mode. Furthermore, the displacement Δ_t of the potential energy minimum along the normal coordinate Q_t is zero for a nontotally symmetric vibrational mode if one assumes that the molecule does not change point groups upon excitation.[1] Note that in eqs 11 and 12 Raman nonresonant terms (see the second term in eq 6) are taken into account, which is omitted in refs 15 and 16 when Warshel et al. studied resonance Raman scattering.

When the electronic wavefunction of the ground state is described by a single Slater determinant that is constructed from the SCF molecular orbitals, ϕ_n and the electronic wavefunction of the excited state is given by $|M\rangle = \sum_n C_n^M \Psi_{n1\rightarrow n2}$ where $\Psi_{n1\rightarrow n2}$ describes a singlet one electron excitation from molecular orbitals ϕ_{n1} to ϕ_{n2}. The derivative of the electric dipole transition moment with respect to normal coordinates in eq 12 can be evaluated in the following way:[15]

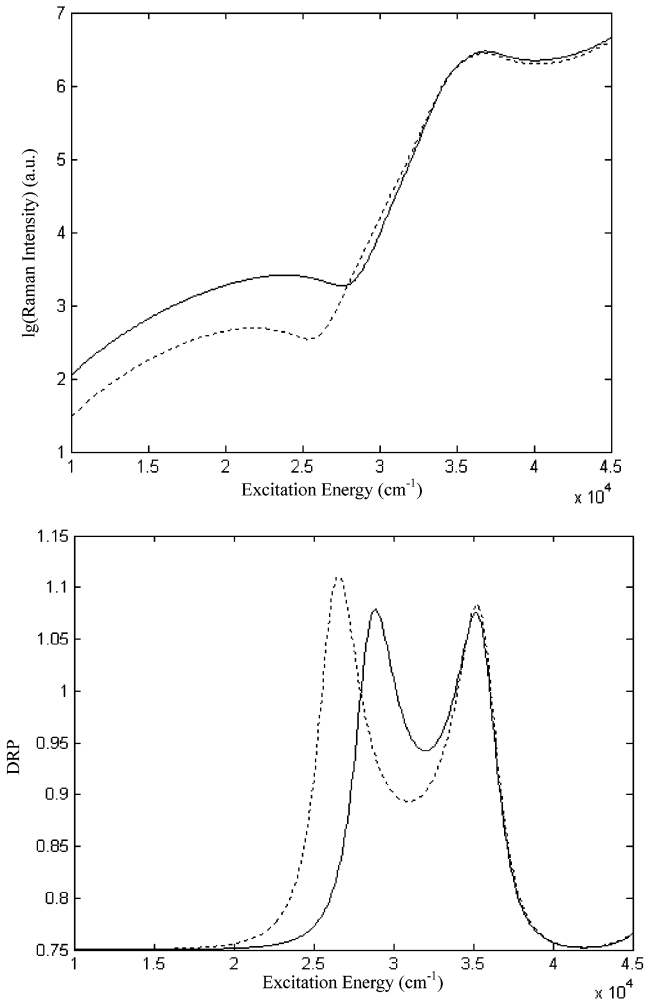

Figure 2. Calculated preresonance excitation profiles and DPR due to Raman resonant and nonresonant terms (solid line) and Raman resonant term (dotted line) of the b_{3g} vibrational mode of naphthalene at 1629 cm^{-1} using the 100-excited-singlet-state model with the damping constant $\Gamma = 1600$ cm^{-1} and the displacement parameter $\Delta_t = 0$.

$$\vec{\mu}_\rho^{\,GM}(\vec{r}) = \langle G|\vec{\mu}|M\rangle_0 = \langle G|e\sum_k (\vec{r}_k)_\rho|M\rangle_0 = \sqrt{2}\sum_n C_n^M\langle\phi_{n1}|e(\vec{r})_\rho|\phi_{n2}\rangle \quad (13)$$

where the coefficients C_n^M are the components of the Mth eigenvector of the configuration interaction matrix and the SCF molecular orbitals ϕ_{n1} and ϕ_{n2} can be expressed into:

$$\phi_n = \sum_i \upsilon_{ni}\lambda_i \quad (14)$$

where υ_{ni} is the coefficient of the atomic orbital λ_i in the molecular orbital n. With use of eq 14, eq 13 gives

$$\vec{\mu}_\rho^{\,GM}(\vec{r}) = \sqrt{2}\sum_{n,i,j} C_n^M\upsilon_{n1i}\upsilon_{n2j}\langle\lambda_i|e(\vec{r}_k)_\rho|\lambda_j\rangle \quad (15)$$

The normal mode vector $\mathscr{R}_s$ defines the transformation between Cartesian coordinates and normal coordinates

$$\mathbf{M}^{1/2}\delta r = \mathscr{R}^M Q^M \quad (16)$$

where M is a diagonal matrix of the atomic masses. When eq 15 is differentiated with respect to normal coordinates while

TABLE 1: Calculated Excited Energies, Electric Dipole Transition Moments (a.u.), Oscillator Strengths, and Electric Dipole Transition Moment Derivatives with Respect to the 1629 cm^{-1} b_{3g} Vibrational Mode for the Excited Singlet States of Naphthalene Molecules with Nonzero Electric Dipole Transition Moments Using the TDDFT//B3LYP/AUG-cc-pVDZ Method

state	excitation energies[a] (cm^{-1})	$\langle i\|x\|0\rangle$	$\langle i\|y\|0\rangle$	$\langle i\|z\|0\rangle$	f	$\partial\mu_x^{GM}/\partial Q_t$	$\partial\mu_y^{GM}/\partial Q_t$	$\partial\mu_z^{GM}/\partial Q_t$
1 (B_{1U})	34708 (34600)	0.0000	0.0000	−0.7120	0.0534	0.0000	−0.0247	0.0000
2 (B_{2U})	35492	0.0000	0.0044	0.0000	0.0000	0.0000	0.0000	0.0002
7 (B_{2U})	46793 (45400)	0.0000	−2.9665	0.0000	1.2508	0.0000	0.0000	−0.0002
8 (B_{3U})	47959	0.3353	0.0000	0.0000	0.0164	0.0000	0.0000	0.0000
9 (B_{1U})	48483	0.0000	0.0000	−1.1084	0.1809	0.0000	0.0220	0.0000
12 (B_{3U})	49097	0.3004	0.0000	0.0000	0.0135	0.0000	0.0000	0.0000
22 (B_{3U})	55054	0.1932	0.0000	0.0000	0.0062	0.0000	0.0000	0.0000
27 (B_{2U})	57606	0.0000	−0.4538	0.0000	0.0360	0.0000	0.0000	0.0008
28 (B_{3U})	58579	−0.1464	0.0000	0.0000	0.0038	0.0000	0.0000	0.0000
30 (B_{1U})	59308	0.0000	0.0000	−0.6513	0.0765	0.0000	−0.0134	0.0000
31 (B_{3U})	59554	0.3764	0.0000	0.0000	0.0256	0.0000	0.0000	0.0000
37 (B_{3U})	60783	0.0495	0.0000	0.0000	0.0005	0.0000	0.0000	0.0000
39 (B_{1U})	61079 (59800)	0.0000	0.0000	−1.5044	0.4199	0.0000	−0.0112	0.0000
40 (B_{3U})	61469	0.1501	0.0000	0.0000	0.0042	0.0000	0.0000	0.0000
45 (B_{1U})	63684	0.0000	0.0000	0.1345	0.0035	0.0000	0.0015	0.0000
50 (B_{2U})	65568	0.0000	0.1283	0.0000	0.0033	0.0000	0.0000	0.0102
52 (B_{3U})	66065	−0.1268	0.0000	0.0000	0.0032	0.0000	0.0000	0.0000
59 (B_{3U})	66950	−0.2982	0.0000	0.0000	0.0181	0.0000	0.0000	0.0000
63 (B_{2U})	67638	0.0000	0.2732	0.0000	0.0153	0.0000	0.0000	−0.0014
66 (B_{3U})	68430	0.2319	0.0000	0.0000	0.0112	0.0000	0.0000	0.0000
67 (B_{3U})	68886	0.1256	0.0000	0.0000	0.0033	0.0000	0.0000	0.0000
68 (B_{2U})	68889	0.0000	−0.1748	0.0000	0.0064	0.0000	0.0000	0.0348
72 (B_{1U})	69156	0.0000	0.0000	0.8132	0.1389	0.0000	−0.0992	0.0000
73 (B_{2U})	69173	0.0000	0.1625	0.0000	0.0056	0.0000	0.0000	−0.0056
76 (B_{3U})	69619	0.1579	0.0000	0.0000	0.0053	0.0000	0.0000	0.0000
80 (B_{1U})	70142	0.0000	0.0000	−0.3633	0.0281	0.0000	−0.0258	0.0000
82 (B_{1U})	70613	0.0000	0.0000	−0.1872	0.0075	0.0000	−0.0735	0.0000
83 (B_{2U})	71108	0.0000	−0.2555	0.0000	0.0141	0.0000	0.0000	0.0240
84 (B_{3U})	71177	0.1008	0.0000	0.0000	0.0022	0.0000	0.0000	0.0000
86 (B_{3U})	72363	−0.0950	0.0000	0.0000	0.0020	0.0000	0.0000	0.0000
89 (B_{2U})	73087	0.0000	−0.0448	0.0000	0.0004	0.0000	0.0000	0.0016
95 (B_{3U})	73691	0.1169	0.0000	0.0000	0.0031	0.0000	0.0000	0.0000
100(B_{3U})	74568	0.1376	0.0000	0.0000	0.0043	0.0000	0.0000	0.0000

[a] Values in the parentheses represent the electronic energies from ref 5.

we hold υ_{n1i} and υ_{n2j} constant, the derivative of the electric dipole transition moment is[15]

$$(\partial\vec{\mu}_\rho^{GM}/\partial Q_t)_0 = (\hbar/2\pi c\upsilon_t)^{1/2}\sum_{n,i,j}\sqrt{2}C_n^M\upsilon_{n1i}\upsilon_{n2j}S_{ij}\mathscr{R}_t^{i\rho}m_i^{-1/2} \tag{17}$$

where $S_{ij} = \langle\lambda_i|\lambda_j\rangle$ is the element of the overlap matrix. When the overlap integrals are taken into account, eq 17 holds even if the atom orbitals are not orthogonalized. Note that in the above Hartree−Fock scheme ϕ_n is the SCF molecule orbital. Only if the SCF molecule orbital in eqs 13 and 14 is replaced by the Kohn−Sham orbital, the density functional theory can also be applied to obtain the electric dipole transition moment and its derivative (eqs 15 and 17).

Using eqs 3, 8, 11, and 12 and molecule symmetry, we can write the Placzek isotropic, antisymmetric, and anisotropy tensor invariants Σ^0, Σ^1, and Σ^2 for the 1629 cm^{-1} b_{3g} vibrational modes of naphthalene molecules into[1,14]

$$\Sigma^0 = 0 \qquad \Sigma^1 = \frac{1}{2}|B_{yz} - B_{zy}|^2 \qquad \Sigma^2 = \frac{1}{2}|B_{yz} + B_{zy}|^2 \tag{18}$$

3. Calculations and Discussion on Preresonance Excitation Profiles and DPR for Naphthalene Molecules

Ehland et al.[4] have measured the polarized Raman excitation spectra of the 1578 cm^{-1} a_{1g} and 1629 cm^{-1} b_{3g} vibrational modes for naphthalene molecules in the preresonance region of the lowest allowed electronic transitions, and the investigated nontotally symmetric mode exhibit a prominent anti-resonance. In this section, we study the anti-resonance phenomenon for this 1629 cm^{-1} b_{3g} mode. First, the structure of naphthalene is optimized, and the corresponding excited states are computed; second, the displacement parameter and the damping constant are determined; third, the anti-resonance excitation profiles and DRP are presented, and the origin of anti-resonance is discussed.

3.1. Structure Optimization and Computations on Excited States. Using the density functional method[24,25] B3LYP and Dunning's correlation consistent basis set[26,27] AUG-cc-pVDZ with the Gaussian 98 program,[28] we perform a geometry optimization and calculate the fundamental frequencies for naphthalene. Then primitive exponents, contraction coefficients and coordinates of each shell for atomic orbitals, Kohn−Sham orbital coefficients, and Hessian matrix of force constants are obtained.

On the basis of optimization, a time-dependent density functional method[29,30] (TDDFT) is applied to compute the excited electronic singlet states and electric dipole transition moments. The electric dipole transition moment derivatives with respect to the 1629 cm^{-1} b_{3g} mode are also computed with use of eq 17. The above results are listed in Table 1. Table 1 shows that the electric dipole transition moment derivatives of the B_{3U} excited singlet states are zero and those of the B_{1U} and B_{2U} excited singlet states are nonzero, which indicates that because of the Raman *B* term only the B_{1U} and B_{2U} singlet excited states contribute to Raman scattering of the 1629 cm^{-1} b_{3g} mode. This agrees with Hassing's discussion[14] from a viewpoint of group theory. The three calculated excited electronic singlet states of

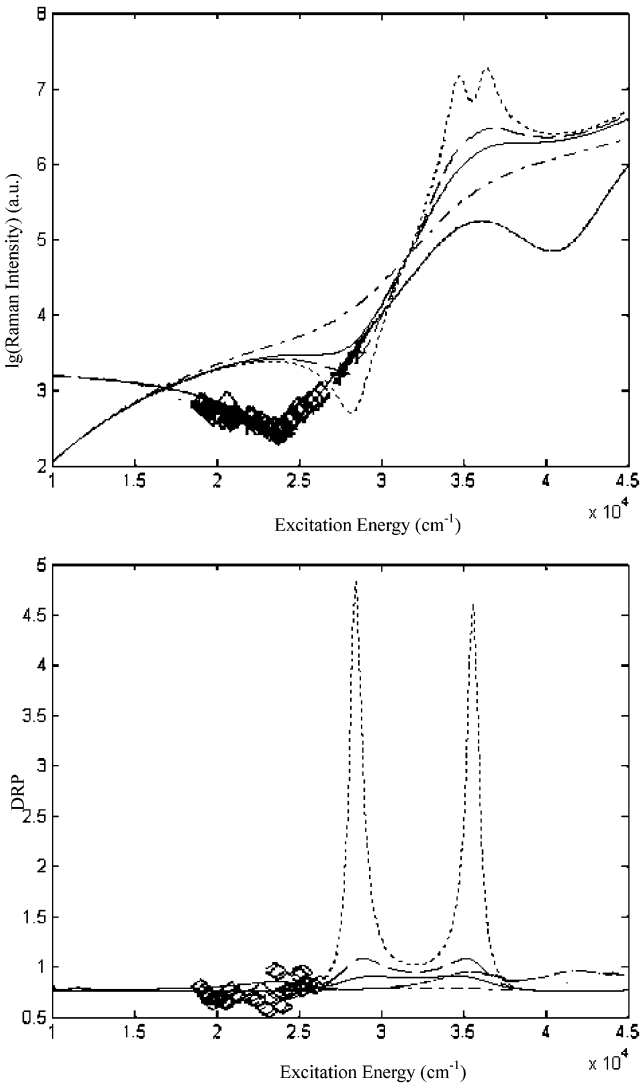

Figure 3. Calculated preresonance excitation profiles and DPR of the b_{3g} vibrational mode of naphthalene at 1629 cm^{-1} using the 100-excited-singlet-state model with the damping constants $\Gamma = 5000$ cm^{-1} (dashed-dotted line), $\Gamma = 2400$cm^{-1} (solid line), $\Gamma = 1600$ cm^{-1} (dashed line), and $\Gamma = 450$ cm^{-1} (dotted line) and the displacement parameter $\Delta_t = 0$. Also, the thin line represents the fit for the preresonance excitation profiles and DPR of this mode using a three-state model of $E_e = 34\,600$ cm^{-1}, $E_{e'} = 45\,400$ cm^{-1}, $E_{e''} = 59\,800$ cm^{-1} (see Table 1 and ref 5) with the cw experimental data (squares) and the excimer data (crosses) from Figure 1 of ref 4.

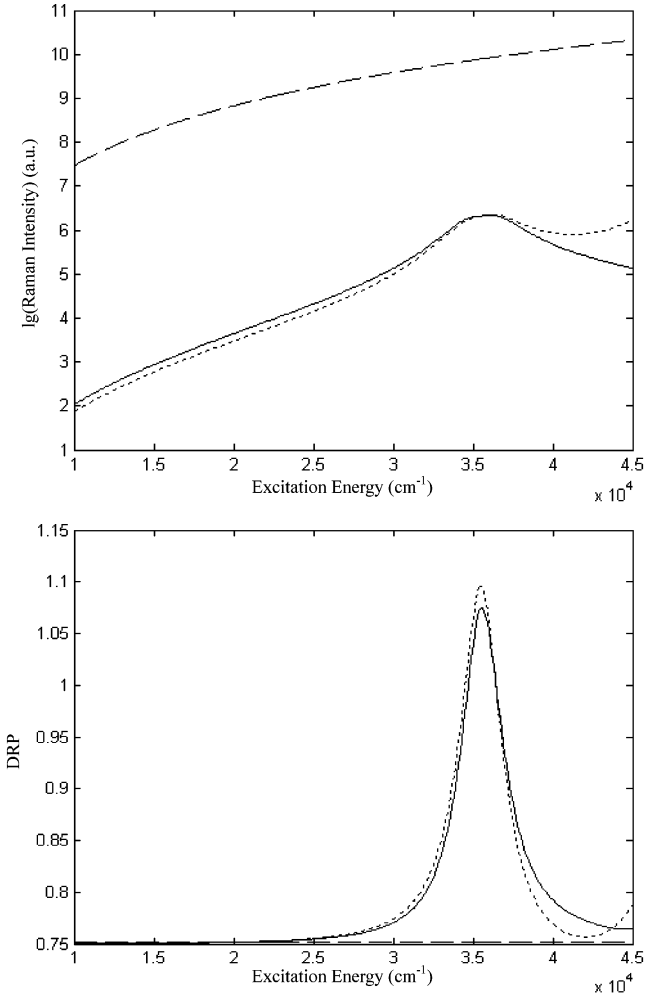

Figure 4. Calculated preresonance excitation profiles and DPR of the b_{3g} vibrational mode of naphthalene at 1629 cm^{-1} using 1-excited-singlet-state model (dashed line), 7-excited-singlet-state model (solid line), and 39-excited-singlet-state model (dotted line) with the damping constant $\Gamma = 1600$ cm^{-1} and the displacement parameter $\Delta_t = 0$.

34 708 cm^{-1} $^1B_{1u}$, 46 793 cm^{-1} $^1B_{2u}$, and 61 079 cm^{-1} $^1B_{1u}$ of naphthalene correspond to the observed excited states of 34 600 cm^{-1} $^1B_{1u}$, 45 400 cm^{-1} $^1B_{2u}$, and 59 800 cm^{-1} $^1B_{1u}$, respectively, by Ohta and Ito[2] (see Table 1). The calculated excitation energies are about 0.3%−2.1% larger than experimental ones. Table 1 also shows that, besides these three excited states, the 72 $^1B_{1U}$ state of 69 156 cm^{-1} is an excited state with a large electric dipole transition moment of 0.8132 a.u. along *z* axes. Furthermore, the derivative of the electric dipole transition moment with respect to the 1629 cm^{-1} b_{3g} vibrational mode of this state with a value of $\partial\mu_y^{GM}/\partial Q_t = -0.0992$ is largest among the 100 excited electronic singlet states.

Note that, in the following anti-resonance computations, the experimental vibrational frequency[4] 1629 cm^{-1} instead of the calculated one 1669 cm^{-1} for the b_{3g} mode is utilized, and the configuration interaction coefficients larger than 0.0001 of the excited electronic singlet states are taken into consideration. The minimum of the configuration interaction coefficients computed by the Gaussian 98 program is 0.0001.

3.2. Parameters in Computations. Applying the 100 excited singlet states (100-excited-singlet-state model) and eqs 1−5, 12, 17, and 18, we discuss how to determine the displacement parameter Δ_t of the potential minimum of the excited states and the damping constant Γ.

The 1629 cm^{-1} b_{3g} mode is a nontotally symmetric vibrational mode, and the displacement along this mode must be zero if the molecule does not change symmetry as a result of the electronic excitation.[1] Also, computational results show that if the molecule changes the point group on excitation, the excitation profiles and DRP of the 1629 cm^{-1} b_{3g} mode are not sensitive to the displacement parameter Δ_t when $\Delta_t \ll 1$ in all of the nonresonant, preresonant, and resonant region. For example, the curves of relative Raman intensities versus excitation energy with $\Delta_t = 0$ and $\Delta_t = 0.2$ are almost superposed, so do DRP (see Figure 1). The reason is that the 1629 cm^{-1} b_{3g} mode is a nontotally symmetry vibrational mode and its Raman scattering is from the Raman *B* term (eq 12). Different from the Raman *A* term (eq 11), the Raman *B* term is insensitive to the displacement parameter Δ_t when the displacement parameter is very small. Thus, all of the displacement parameters of the excited states for the 1629 cm^{-1} b_{3g} mode are taken to be zero for simplification.

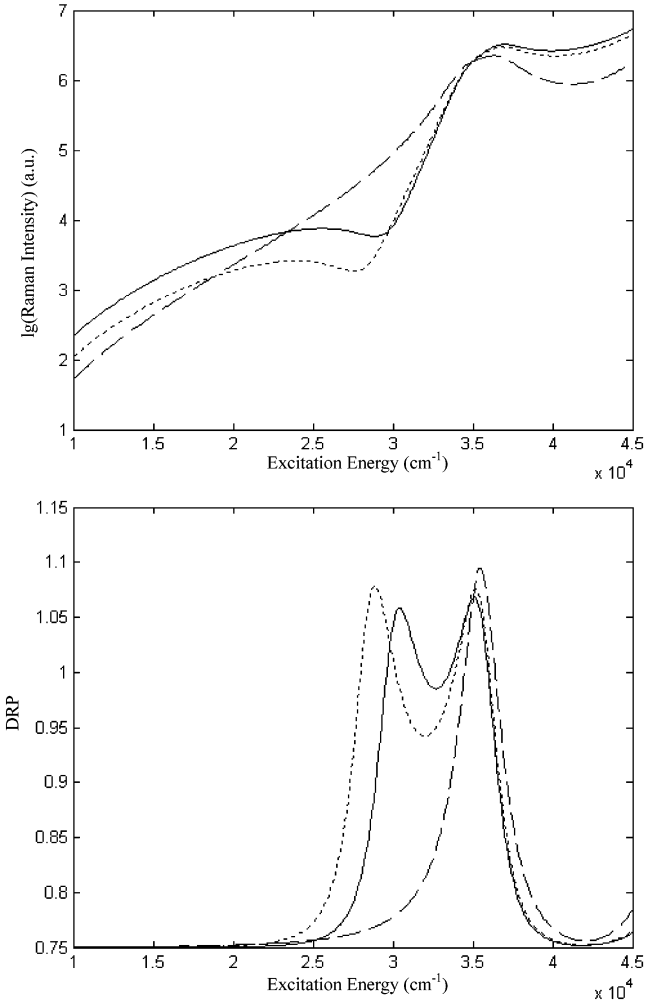

Figure 5. Calculated preresonance excitation profiles and DPR of the b_{3g} vibrational mode of naphthalene at 1629 cm^{-1} using 71-excited-singlet-state model (dashed line), 72-excited-singlet-state model (solid line), and 100-excited-singlet-state model (dotted line) with the damping constant $\Gamma = 1600$ cm^{-1} and the displacement parameter $\Delta_t = 0$.

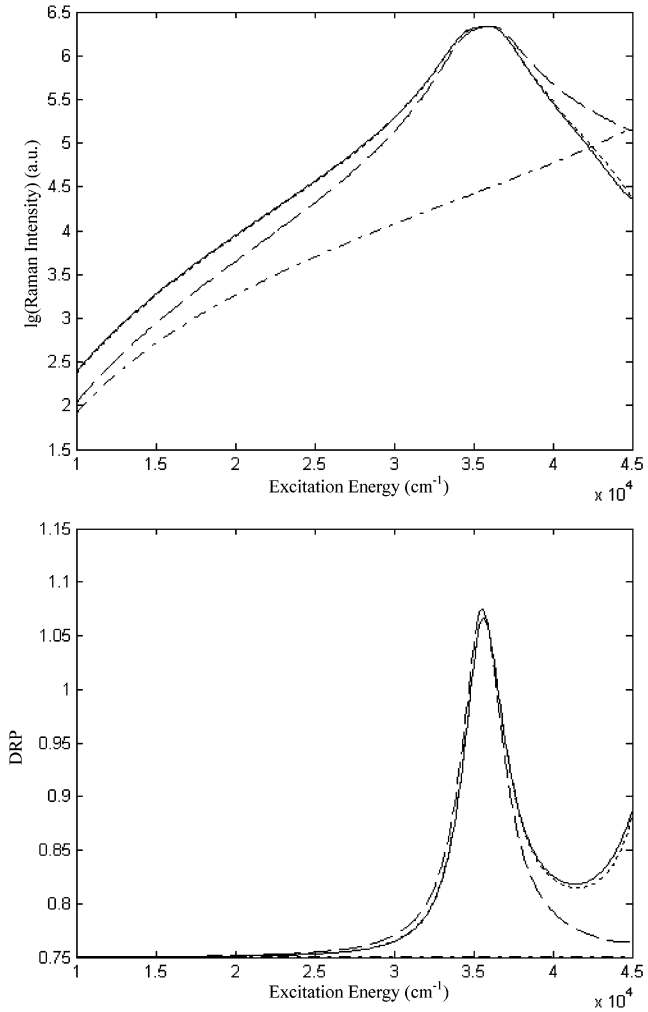

Figure 6. Calculated preresonance excitation profiles of the b_{3g} vibrational mode of naphthalene at 1629 cm^{-1} using the 1- and 7-excited-singlet-state model (dashed line), 1- and 39-excited-singlet-state model (dotted line), 7- and 39-excited-singlet-state model (dashed-dotted line), and 1-, 7-, and 39-excited-singlet-state model (solid line) with the damping constant $\Gamma = 1600$ cm^{-1} and the displacement parameter $\Delta_t = 0$.

Figure 2 shows that the excitation profiles and DPR in the preresonant region due to both the Raman resonant term (see the first term in eq 6) and the Raman nonresonant term (see the second term in eq 6) are different from those only due to the Raman resonant term. This indicates that the Raman nonresonant term influences preresonance Raman scattering though it does not in resonance Raman scattering. Hence, both Raman resonant and nonresonant terms should be taken into account in the preresonance study.

The preresonant excitation profiles and DPR of the 1629 cm^{-1} b_{3g} mode with the damping constants $\Gamma = 5000$ cm, $\Gamma = 2400$ cm^{-1}, $\Gamma = 1600$ cm^{-1}, and $\Gamma = 450$ cm^{-1} are computed, respectively, which are displayed in Figure 3. Figure 3 shows that the damping constant has an influence on the preresonant excitation profiles and DPR, and the dispersion of DRP in the anti-resonant region decreases when the damping constant increases. Figure 1 in ref 4 shows that there is a very weak dispersion of DRP in the preresonant region for the 1629 cm^{-1} b_{3g} mode: the minimum of the DRP is 0.50 and the maximum of the DRP is 0.85. The calculated dispersion of DRP with the damping constants $\Gamma = 5000$ cm^{-1}, $\Gamma = 2400$ cm^{-1}, $\Gamma = 1600$ cm^{-1}, and $\Gamma = 450$ cm^{-1} are in the range of 0.75−0.78, 0.75−0.91, 0.75−1.1, and 0.75−4.8, respectively (see Figure 3). All DRP show weak dispersion except that with $\Gamma = 450$ cm^{-1}. However, no anti-resonance can be observed when the damping constant is taken to be too large ($\Gamma = 5000$ cm^{-1}). Figure 3 also shows that, when the damping constants are 450 cm^{-1}, 1600 cm^{-1}, and 2400 cm^{-1}, the corresponding anti-resonance minimum energies where the relative Raman intensity has a minimum in the preresonant region are 28 200 cm^{-1}, 27 600 cm^{-1}, and 25 900 cm^{-1} , respectively. Figure 1 in ref 4 shows that the experimental anti-resonance minimum energy is about 23 600 cm^{-1}. The calculated anti-resonance minimum energies with $\Gamma = 450$ cm^{-1}, $\Gamma = 1600$ cm^{-1}, and $\Gamma = 2400$ cm^{-1} are about 19%, 17%, and 9.7% larger than the experimental data,[4] respectively. Also, the difference of the minimum energy between experiment and computations decreases with the increasing damping constants. Generally, both the calculated DRP and the anti-resonance minimum energy are a little larger than experiment.[4] One reason may be that the anti-resonance is an interference effect, which is very sensitive to even small changes in the vibronic parameters such as the transition moments and their first derivatives, and it is not so easy to obtain sufficiently accurate values for the vibronic parameters although the time-dependent density functional method and Warshel et al.'s calculation method of electric dipole transition moment derivatives are excellent; the other reason may be that the calculated naphthalene molecule is in vacuum and the experi-

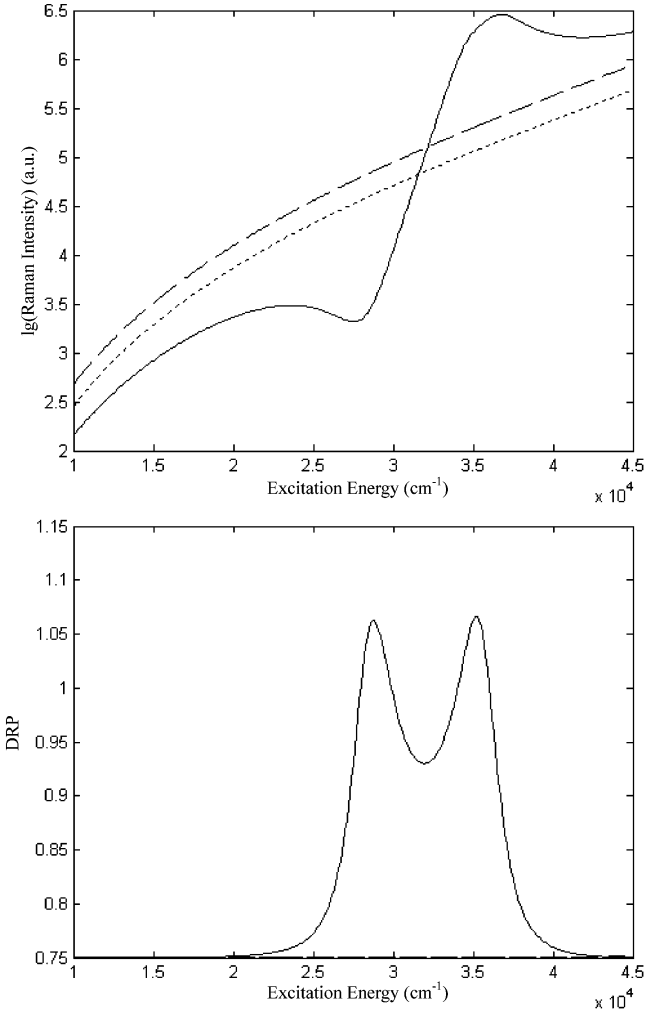

Figure 7. Calculated preresonance excitation profiles of the b_{3g} vibrational mode of naphthalene at 1629 cm^{-1} using the 1- and 72-excited-singlet-state model (solid line), 7- and 72-excited-singlet-state model (dotted line), and 39- and 72-excited-singlet-state model (dashed-dotted line) with the damping constant $\Gamma = 1600$ cm^{-1} and the displacement parameter $\Delta_t = 0$.

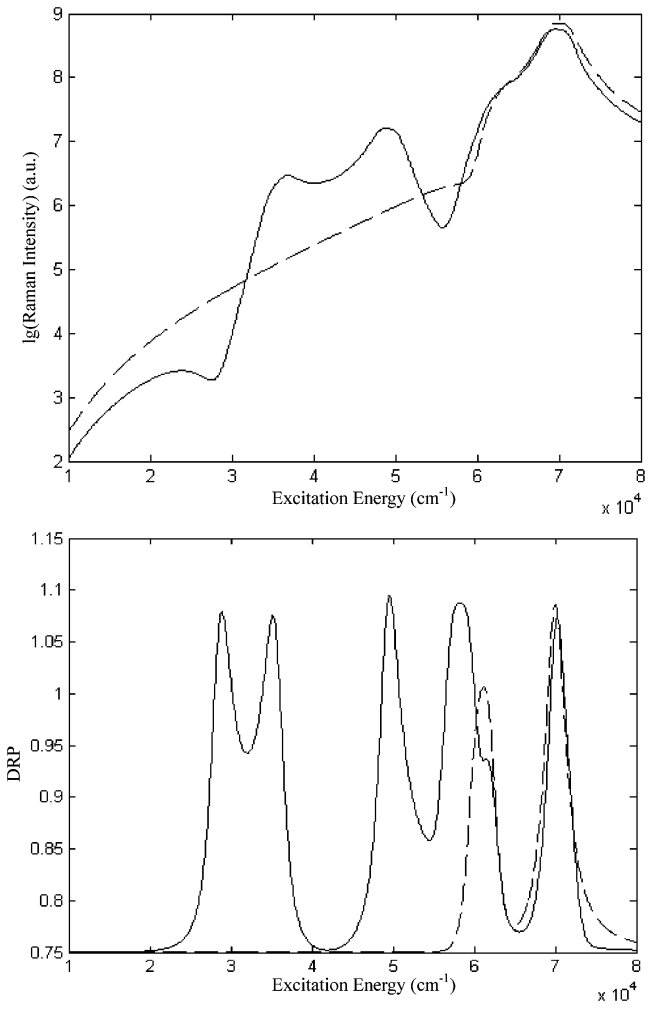

Figure 8. Calculated resonance excitation profiles of the b_{3g} vibrational mode of naphthalene at 1629 cm^{-1} using the 39- and 72-excited-singlet-state model (dashed line) and 100-excited-singlet-state model (solid line) with the damping constant $\Gamma = 1600$ cm^{-1} and the displacement parameter $\Delta_t = 0$.

ment[4] is conducted in solution where the interaction between the solvent and the solute have an influence not only on excitation energies but also on electric dipole transition moments and their derivatives. Theoretically, all of the damping constants of the different excited vibronic states are different from each other, and for convenience, all of the damping constants of the excited vibronic states are assumed to be 1600 cm^{-1}, except where otherwise stated.

3.3. Origin of Anti-resonance Raman Scattering. In order to investigate the origin of anti-resonance phenomenon of the b_{3g} vibrational mode of naphthalene at 1629 cm^{-1}, we compute its preresonant excitation profiles and DPR using the 1-excited-singlet-state model, 7-excited-singlet-state model, 39-excited-singlet-state model, 71-excited-singlet-state model, 72-excited-singlet-state model, and 100-excited-singlet-state model, respectively. The results are plotted in Figures 4 and 5. From these two figures, some results can be obtained as follows: (i) no anti-resonance phenomenon of the 1629 cm^{-1} b_{3g} mode can be observed when only the first excited singlet state 1^1B_{1U} are considered, which indicates that the anti-resonance phenomenon is not arising from the interference between the 0−0 and 0−1 fundamental Raman transitions of the 1^1B_{1U} excitation state. (ii) No anti-resonance phenomenon appears when the 7-excited-singlet-state model, 39-excited-singlet-state model, and 71-excited-singlet-state model are applied although Raman intensities from these states are about 4−5 orders of magnitude smaller than those only from the 1^1B_{1U} single state, which indicates there is a destructive interference between these excited electronic states. Further computations indicate that no anti-resonance phenomenon can be observed (see Figure 6) when only the 1^1B_{1U} and 7^1B_{2U} states, 1^1B_{1U} and 39^1B_{1U} states, 7^1B_{2U} and 39^1B_{1U} states, and 1^1B_{1U}, 7^1B_{2U}, and 39^1B_{1U} states are taken into consideration, respectively. This indicates that the interaction between the 1^1B_{1U}, the 7^1B_{2U}, and the 39^1B_{1U} states is not the origin of anti-resonance of the 1629 cm^{-1} b_{3g} mode. (iii) Anti-resonance phenomenon in the preresonant region appears when the 72-excited-state model is used. Further computations show (see Figure 7) that there is an anti-resonance when only the 1^1B_{1U} and 72^1B_{1U} states are considered, and the interaction between these two states is a destructive interference where Raman intensities from them around their anti-resonance minimum energy are about 6 orders of magnitude smaller than those from the 1^1B_{1U} state. In the preresonant region, no anti-resonance can be observed between the 7^1B_{2U} and the 72^1B_{1U} states, as well as the 39^1B_{1U} and 72^1B_{1U} states (see also Figure 7). (iv) When the 100-excited-singlet-state model is considered, the preresonant excitation profiles and anti-resonance minimum energy become a little smaller, and the dispersion of DRP becomes a little stronger.

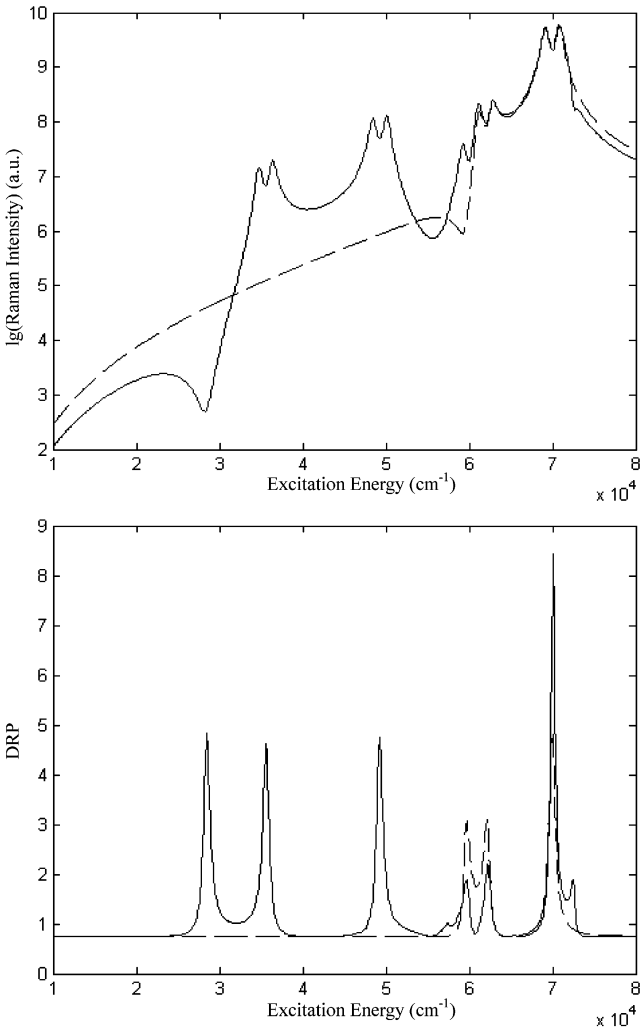

Figure 9. Calculated resonance excitation profiles of the b_{3g} vibrational mode of naphthalene at 1629 cm^{-1} using the 39- and 72-excited-singlet-state model (dashed line) and 100-excited-singlet-state model (solid line) with the damping constant $\Gamma = 450$ cm^{-1} and the displacement parameter $\Delta_t = 0$.

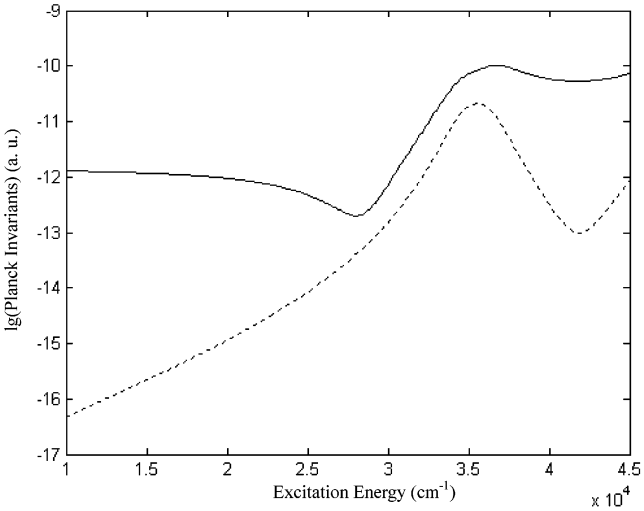

Figure 10. Calculated antisymmetric invariants Σ^1 (solid line) and anisotropic invariants Σ^2 (dotted line) versus excitation frequency in the preresonant region of the b_{3g} vibrational mode of naphthalene at 1629 cm^{-1} using the 100-excited-singlet-state model with the damping constant $\Gamma = 1600$ cm^{-1} and the displacement parameter $\Delta_t = 0$.

From the above discussions, we can come to a conclusion that the origin of the anti-resonance for the 1629 cm^{-1} b_{3g} mode of naphthalene in the preresonant region is the destructive interference between the 1^1B_{1U} and the 72^1B_{1U} electronic states.

It is noted that, in the resonant region, anti-resonance phenomenon appears with the anti-resonance minimum energy of about 60 000 cm^{-1} when the damping constant is taken to 450 cm^{-1} instead of 1600 cm^{-1} (see Figures 8 and 9) though there is no anti-resonance between the 39^1B_{1U} and the 72^1B_{1U} states in the preresonant region. However, when the 100-excited-singlet-state model is used, this anti-resonance is smeared out by resonance Raman scattering.

Also, antisymmetric and anisotropic tensor invariants of the 1629 cm^{-1} b_{3g} mode are computed (see Figure 10). Figure 10 shows a pronounced anti-resonance of antisymmetric invariants in the preresonant region.

4. Conclusions

The anti-resonance phenomenon in Raman scattering is investigated in the preresonance region on the basis of the direct Taylor expansion of the electric dipole transition moments in vibrational Raman transition polarizabilities with respect to vibrational normal coordinates. Using the deduced formulas and a time-dependent density functional theory study on the excited electronic states of naphthalene molecules, the anti-resonance of the nontotally symmetric b_{3g} vibrational model at 1629 cm^{-1} is calculated and its origin is discussed, the model spectra compare favorably with experiment. This direct evaluation approach may provide a method of predicting anti-resonance and studying its origin.

References and Notes

(1) Mortensen, O. S.; Hassing, S. *Adv. Infrared Raman Spectrosc.* **1980**, *6*, 1.
(2) Ohta, N.; Ito, M. *Chem. Phys.* **1977**, *20*, 71.
(3) Aminzadeh, A.; Fawcett, V.; Long, D. A. *J. Raman Spectrosc.* **1980**, *9*, 214.
(4) Ehland, F.; Hassing, S.; Dreybrodt, W. *J. Raman Spectrosc.* **1999**, *30*, 537.
(5) Schmid, E. D.; Derner, H.; Berthold, G. *J. Raman Spectrosc.* **1975**, *4*, 329.
(6) Stein, P.; Miskowski, V.; Woodruff, W. H.; Griffin, J. P.; Werner, K. G.; Gaber, B. P.; Spiro, T. G. *J. Chem. Phys.* **1976**, *64*, 2159.
(7) Ziegler, L. D.; Albrecht, A. C. *J. Chem. Phys.* **1979**, *70*, 2634.
(8) Okamoto, H.; Hamaguchi, H.; Tasumi, M. *Chem. Phys. Lett.* **1986**, *130*, 185.
(9) Kosmidis, C.; Bolovinos, A.; Tsekeris, P. *J. Raman Spectrosc.* **1990**, *21*, 737.
(10) Zgierski, M. Z. *J. Raman Spectrosc.* **1977**, *6*, 53.
(11) Dirac, P. A. M. *The principles of quantum mechanics;* Oxford University Press: London, 1958.
(12) Robinson, G. W.; Auerbach, R. A. *J. Chem. Phys.* **1981**, *74*, 2083.
(13) Hassing, S.; Svendsen, E. N. *Chem. Phys. Lett.* **1982**, *86*, 342.
(14) Hassing, S. *J. Raman Spectrosc.* **1997**, *28*, 739.
(15) Warshel, A.; Dauber, P. *J. Chem. Phys.* **1977**, *66*, 5477.
(16) Warshel, A. *Annu. Rev. Biophys. Bioeng.* **1977**, *6*, 273.
(17) Warshel, A. *Chem. Phys. Lett.* **1976**, *43*, 273.
(18) Liang, R.; Schnepp, O.; Warshel, A. *Chem. Phys. Lett.* **1976**, *44*, 394.
(19) Albrecht, A. C. *J. Chem. Phys.* **1961**, *34*, 1476.
(20) Hassing, S.; Svendsen, E. N. *J. Raman Spectrosc.* **2004**, *35*, 87.
(21) Liu, F.-C. *J. Phys. Chem.* **1991**, *95*, 7180.
(22) Liu, F.-C.; Buckingham, A. D. *Chem. Phys. Lett.* **1993**, *207*, 325.
(23) Manneback, C. *Physica* **1951**, *11*, 1001.
(24) Lee, C.; Yang, W.; Parr, R. G. *Phy. Rev. B* **1988**, *37*, 785.
(25) Becke, A. D. *J. Chem. Phys.* **1993**, *98*, 5648.
(26) Kendall, R. A.; Dunning, T. H., Jr.; Harrison, R. J. *J. Chem. Phys.* **1992**, *96*, 6796.
(27) Dunning, T. H., Jr. *J. Chem. Phys.* **1989**, *90*, 1007.
(28) Frisch, M. J.; Trucks, G. W.; Schlegel, H. B.; Scuseria, G. E.; Robb, M. A.; Cheeseman, J. R.; Zakrzewski, V. G.; Montgomery, J. A., Jr.; Stratmann, R. E.; Burant, J. C.; Dapprich, S.; Millam, J. M.; Daniels, A. D.; Kudin, K. N.; Strain, M. C.; Farkas, O.; Tomasi, J.; Barone, V.; Cossi,

M.; Cammi, R.; Mennucci, B.; Pomelli, C.; Adamo, C.; Clifford, S.; Ochterski, J.; Petersson, G. A.; Ayala, P. Y.; Cui, Q.; Morokuma, K.; Malick, D. K.; Rabuck, A. D.; Raghavachari, K.; Foresman, J. B.; Cioslowski, J.; Ortiz, J. V.; Stefanov, B. B.; Liu, G.; Liashenko, A.; Piskorz, P.; Komaromi, I.; Gomperts, R.; Martin, R. L.; Fox, D. J.; Keith, T.; Al-Laham, M. A.; Peng, C. Y.; Nanayakkara, A.; Gonzalez, C.; Challacombe, M.; Gill, P. M. W.; Johnson, B. G.; Chen, W.; Wong, M. W.; Andres, J. L.; Head-Gordon, M.; Replogle, E. S.; Pople, J. A. *Gaussian 98*, revision A.11; Gaussian, Inc.: Pittsburgh, PA, 1998.

(29) Bauernschmitt, R.; Ahlrichs, R. *Chem. Phys. Lett.* **1996**, *256*, 454.

(30) Casida, M. E.; Jamorski, C.; Casida, K. C.; Salahub, D. R. *J. Chem. Phys.* **1998,** *108*, 4439.